Bioremediation Journal
Publication details, including instructions for authors and subscription information:
http://www.tandfonline.com/loi/bbrm20

A Novel Microbial Biofilm for Bioremoval of Nickel from Aqueous Media

Mihiri Seneviratne[a], Meththika Vithanage[b], H. M. S. P. Madawala[c] & Gamini Seneviratne[a]

[a] Microbial Biotechnology Unit, Institute of Fundamental Studies, Kandy, Sri Lanka

[b] Chemical and Environmental Systems Modeling Research Group, Institute of Fundamental Studies, Kandy, Sri Lanka

[c] Department of Botany, University of Peradeniya, Peradeniya, Sri Lanka

Published online: 07 Aug 2015.

To cite this article: Mihiri Seneviratne, Meththika Vithanage, H. M. S. P. Madawala & Gamini Seneviratne (2015) A Novel Microbial Biofilm for Bioremoval of Nickel from Aqueous Media, Bioremediation Journal, 19:3, 239-248, DOI: 10.1080/10889868.2014.995374

To link to this article: http://dx.doi.org/10.1080/10889868.2014.995374

Bioremediation Journal, 19(3):239–248, 2015

ISSN: 1088-9868 print / 1547-6529 online
DOI: 10.1080/10889868.2014.995374

A Novel Microbial Biofilm for Bioremoval of Nickel from Aqueous Media

Mihiri Seneviratne,[1] Meththika Vithanage,[2] H. M. S. P. Madawala,[3] and Gamini Seneviratne [1]
[1]Microbial Biotechnology Unit, Institute of Fundamental Studies, Kandy, Sri Lanka
[2]Chemical and Environmental Systems Modeling Research Group, Institute of Fundamental Studies, Kandy, Sri Lanka
[3]Department of Botany, University of Peradeniya, Peradeniya, Sri Lanka

ABSTRACT This study evaluated the efficacy of a microbial biofilm in removing Ni ions in aqueous media. The biofilm was developed incorporating a garden soil fungus with a bacterium isolated from Ni-rich serpentinite soil. The biofilm was characterized using microscopy, scanning electron microscopy, Fourier transform infrared (FTIR) investigations, and Boehm and potentiometric titrations. Ni removal was determined using batch experiments as a function of pH, Ni concentration, and time. The adsorption isotherm assay was conducted with varying Ni concentrations from 25 to 500 mg/L for 4 days. Isotherm and kinetic modeling were applied to the experimental data to understand the mechanisms of Ni removal. The zero point charge at pH 4.5 indicated the pH values greater than 4.5 is favorable for Ni adsorption. Acidic nature of the biofilm was reflected from Boehm titration data showing higher number of acidic groups than basic groups. With the increase in initial Ni concentration, the uptake increased from 3.43 to 38.16 mg/g. Hill, the best-fitted isotherm model, indicated a maximum adsorption capacity of 165.37 mg/g. After 4 days, the adsorption rate reached an equilibrium with a maximum sorption of ~30 mg/g for an initial concentration of 100 mg/L. Kinetic model fitting with Power function further demonstrated the chemisorptive interaction of Ni with the biofilm surface. A clear involvement of functional groups of the biofilm in Ni bonding was observed from the attenuated total reflection (ATR)-FTIR spectrum. The microbial biofilm showed an efficient but slow removal of Ni from aqueous media.

KEYWORDS FTIR, fungal-bacterial biofilm, isotherm, kinetics, nickel

INTRODUCTION

Bioremoval of heavy metal ions through biosorption is considered as one of the best approaches in metal ion remediation in wastewater. In relation to the cost and skilled operations involved in other processes, bioremoval is an eco-friendly regenerative process with a higher efficiency. Biosorption is a process that involves the use of biological materials to form complexes with metal ions using their functional groups (Krishnani et al. 2008).

Many different agricultural wastes such as peanut husk, rice husk, wheat bran and sawdust, activated carbon, and biochar have been used as potential

Address correspondence to Meththika Vithanage, Chemical and Environmental Systems Modeling Research Group, Institute of Fundamental Studies, Hantana Rd, 20000 Kandy, Sri Lanka. E-mail: meththikavithanage@gmail.com

Color versions of one or more of the figures in the article can be found online at www.tandfonline.com/bbrm.

biosorbents for removal of heavy metals (Hegazi 2013; Trakal et al. 2014; Sewwandi et al. 2012). Even though they are economically favorable, they pose a question for safe disposal. However, conventional bioremediation techniques are incapable of removing high concentrations of metal ions in dynamic systems such as wastewater (Sewwandi et al. 2012). Thus, a regenerating system with high bioremoval capacity for heavy metal ions is an urgent need for the industries. At the moment, the use of biofilms in soil and water remediation is considered as a newly emerging field (Corcoll et al. 2012; Ferris et al. 1989).

Biofilm is a community of microorganisms enclosed with extracellular polymeric substances (EPS) (Seneviratne et al. 2008). The EPS is a complex mixture of macromolecular polyelectrolytes including polysaccharides, proteins, and nucleic acids (Omoike and Chorover 2004). These EPS building molecules contain ionizable functional groups such as carboxyl, phosphoric, amine, and hydroxyl groups (Haghseresht and Lu 1998). Therefore, they display a considerable sorption capacity to most positively charged metal cations, leading to reduced metal transport (Liu, Lam, and Fang 2001; Ngwenya, Sutherland, and Kennedy 2003; Texier, Andrès, and Le Cloirec 1999; Yee and Fein 2001). The adhesion to surfaces and binding organic and inorganic ions through physical and chemical sorption are two key functions of EPS that supports the biosorption processes (Liu, Lam, and Fang 2001).

Many studies have reported successful heavy metal removal by using different monoculture bacterial biofilms (Quintelas, Fonseca et al. 2009; Quintelas, Rocha et al. 2009; Toner et al. 2005). Fungal-bacterial biofilms (FBBs) are more apparent in the field of biofilms as biofertilizers (Seneviratne et al. 2009). Furthermore, they have shown a potential to be used in wastewater reactors for heavy metal remediation purposes (Herath et al. 2013). Studies have shown that the performance of the fungal-bacterial biofilms are higher than that of the mono- or mixed cultures of bacterial biofilms (Herath et al. 2013). Among the heavy metals found in wastewaters, Ni is one of the frequently detected in battery (Jadhav and Hocheng 2013), electroplating, and Zn-based casting industries (Periasamy and Namasivayam 1995). Discharge of these wastewaters without proper treatment may release excessive concentrations of Ni ions into the surrounding environment. Hence, this work aims to develop a Ni-resistant fungal-bacterial biofilm (FBB) to investigate the bioremoval behavior of Ni in aqueous solutions.

METHODOLOGY

Biofilm Formation

Serpentine soils are known to provide a hostile habitat for plant growth and productivity, mainly due to the presence of high levels of trace metals, such as Ni, Cr, and Co (Alves et al. 2011). Serpentine soils in Wasgamuwa, Sri Lanka, were used in this study to isolate the bacterium. Nickel concentration in serpentine soils was found to be more than 6000 mg/kg (Vithanage et al. 2014). Nickel-resistant bacteria were isolated in NA (nutrient agar) from serpentine soil in Wasgamuwa. Each bacterium was coupled with an *Aspergillus* sp. fungus as a carrier in a low-nutrition medium incorporated with czapex dox (CZ) and allowed to form fungal-bacterial biofilms in a rotatry shaker. Initial screening of different fungi from garden soil showed that the *Aspergillus* sp. was the best for biofilm formation and Ni adsorption for the selected bacteria. Here, we focused on garden soil fungi, as in the case of this biofilm they are considered as the carrier for the bacteria. The biofilms were observed through microscope and were screened for Ni adsorption with a Ni concentration series (25, 50, 75, 100, 200, 300, and 500 mg/L). The selected biofilm was used for further Ni adsorption studies.

Potentiometric Titration

One gram of the FBB was equilibrated well at the desired ionic strength for 24 h. Prior to the equilibration and also throughout the titration, the sample was purged with pure N_2 (99.996%) to minimize CO_2 contaminations. Three titration experiments were performed on the basis of different electrolytic concentrations (0.1, 0.01, and 0.001 M $NaNO_3$). The initial pH of FBB suspension was approximately 4, and it was raised to 9 with 0.0989 M NaOH before the titration commenced. The surface charge (σ_H) was calculated using Equation 1.

$$\sigma_H = \frac{(C_A - C_B + [OH^-] - [H^+])}{a} \quad (1)$$

where σ_H is the surface charge (C m^{-2}), C_A is the added acid concentration, C_B is the added base concentration,

$[OH^-]$ is the hydroxyl ion concentration, $[H^+]$ is the proton concentration, a is equilibrium OH^- and H^+ concentrations for a given quantity of solid used ($g\,L^{-1}$),

Boehm Titration

The Boehm titration method (Oh and Yum 2004) was used to determine the surface functional groups containing oxygen. The procedure was modified as in Goertzen et al. (2010) to avoid CO_2 contaminations, reducing its effect on the endpoint. A suspension of FBB (1 g) with 0.05 M sodium hydroxide, sodium carbonate, sodium bicarbonate, and hydrochloric acid were prepared, shaken for 3 h, and the filtrate was titrated for the remaining acid or base concentrations in the solution with an autotitrator (Orion 940 autochemistry analyzer; MA, USA). Before the titration, the samples were degasified for 30 min and titrated immediately while continuing degassing during the titration. The various free acidic groups were derived assuming that NaOH neutralizes carboxylic, lactonic, and phenolic groups; Na_2CO_3 neutralizes carboxylic and lactonic groups; and $NaHCO_3$ neutralizes only carboxylic groups (Goertzen et al. 2010). The quantity of the different possible surface groups were calculated through the difference in the calculated amount of surface functionality that reacted (nCSF) as given in Equation 2:

$$n\text{CSF} = [\text{B}]\,V_\text{B} - [\text{HC1}]\,V_\text{HC1} \cdot V_\text{B}/V_\text{a} \qquad (2)$$

where nCSF = moles of carbon surface functionalities on the surface of BF (μmol g^{-1}); [B], V_B = concentration and volume of the base mixed with BF; V_a = volume of aliquot taken from the V_B; [HCl], V_HCl = concentration and volume of acid added to the V_a.

Biosorption Edges

The pH is one of the most important factors, since hydrogen ions themselves are strongly competing with cationic metal ions, and it also determines the valence state of the ions and their precipitation process. A pH range between 3 and 9 was used in this experiment with 500 mg/L Ni concentration. Acids, bases, and stock solutions were prepared in deionized, distilled water. Precalibrated acids and base solutions of 0.0989 M NaOH and 0.1073 M HNO_3 were used for pH adjustments.

Biosorption Isotherm Assays

Batch experiments were conducted using 1 g of the fungal-bacterial biofilm in 50 ml of different concentrations of heavy metal solutions (25, 50, 100, 200, 300, 500, 750, and 1000 mg/L) in 100-ml Erlenmeyer flasks. The pH of the solutions was measured before and after the sorption. The Erlenmeyer flasks were kept at 35°C, with moderate stirring for 4 days. Samples were filtered through 0.45-mm cellulose acetate filter papers and analyzed for Ni using atomic absorption spectrophotometry (GBC 933AA; NSW, Australia).

ATR-FTIR Investigations

Infrared spectra of both the biofilm and the metal loaded biofilm were obtained using a Fourier transform infrared (FTIR) spectrometer (Nicolet 6700; MA, USA). For the FTIR study, biofilm was centrifuged and dried, followed by weighing. Then attenuated total reflection FTIR (ATR-FTIR) was conducted with finely ground biomass.

RESULTS AND DISCUSSION

Biofilm Formation

About 1 g of the FBB was formed in 5 days. The microscopic (under the oil immersion lens of the microscope and the scanning electron microscope) observations clearly showed that the fungal mycelium was colonized with the bacterial cells (Figure 1). In general, microbial biofilms are formed adherent to biotic or abiotic surfaces (Seneviratne, Weerasekara, and Zavahir 2010). It was noticed that in this case, the fungal mycelium acts as the attaching surface for the bacteria (Figure 1a).

Potentiometric Titrations

The surface charge of the adsorbent could be considered as one of the parameters that affect the adsorption process. Potentiometric titration data revealed the pH range in which FBB surface can adsorb and desorb protons from the solution (Figure 2). The zero point charge (pH_{zpc}) of the biofilm was observed at the pH

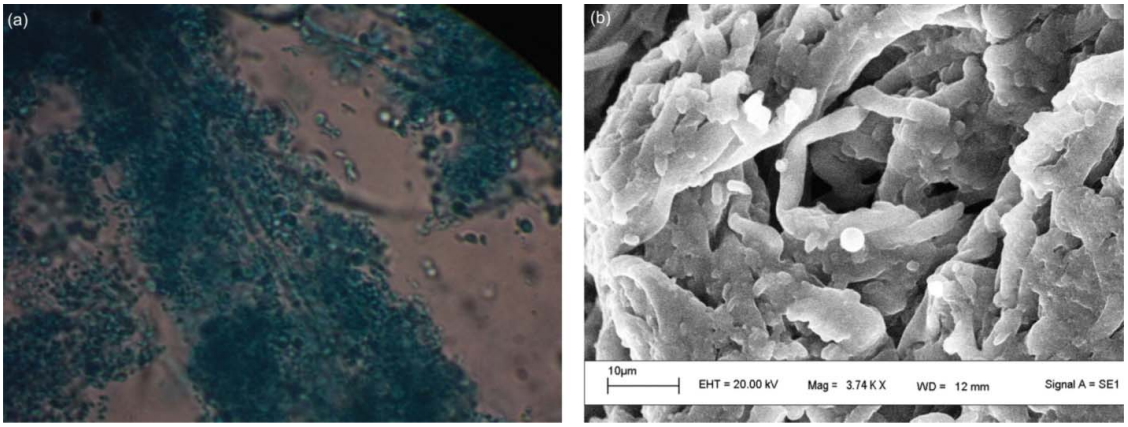

FIGURE 1 (*a*) Light microscopic image of the fungal mycelium colonized by bacterial cells of the microbial biofilm. (*b*) Scanning electron micrograph of the microbial biofilm.

of 4.55, indicating that the biofilm surface becomes negatively charged when the pH value is higher than 4.55. There the surface has a net negative or anionic charge, and the surface would participate in cation attraction and cation-exchange reactions. When the pH is less than zero point charge, the surface has a net positive charge; therefore, the surface will attract anions and participate in anion-exchange reactions. It reflects that the cation adsorption is favorable at pH values greater than 4.55. As observed in the adsorption edge data, the Ni adsorption has increased as the solution pH value increases. Since the zero point charge is 4.55, Ni adsorption is favorable at pH values greater than pH_{zpc}. Therefore, under the pH values of the natural environment, this biofilm is capable of adsorbing Ni ions from aqueous solutions. Furthermore, this biofilm potentially be used to remediate the heavy metal contaminated waters without changing the pH of the media.

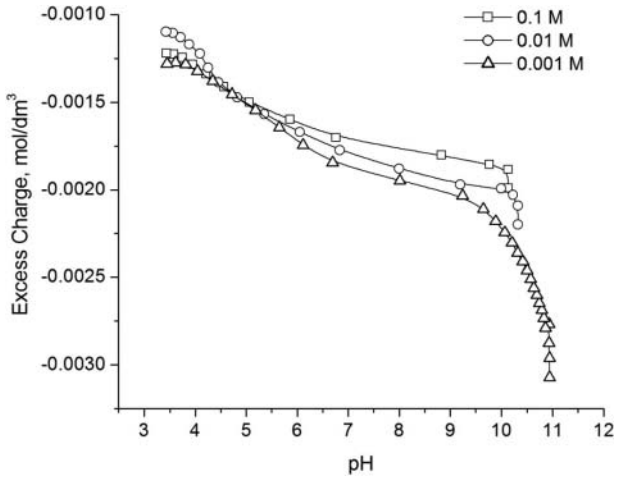

FIGURE 2 Variation of surface charge with pH based on three different ionic strengths. Symbols represent experimental data; solid lines represent model calculations. Titration ranged from pH 4 to 9 and $pH_{zpc} = 4.5$.

Boehm Titration

The surface functional groups of the biofilm were examined and quantified by standard Boehm titration under an inert environment (Goertzen et al. 2010). Different surface functional groups in the biofilm are presented in Table 1. The FBB consisted of high concentration of acidic groups than the basic groups (2702 and 1994 μmol g^{-1}, respectively). Among the acidic sites, the biofilm was rich in phenolic groups, which are about 40 times higher than that of the carboxylic groups. Based on the Boehm quantification, the acidic groups were increased in the order of carboxylic < lactonic < phenolic groups (Table 1).

Adsorption Edges

The influence of the solution pH on the equilibrium Ni uptake levels of the biofilm was determined for different pH values below the Ni precipitation limit. The results indicated that the Ni adsorption was high at low pH levels; at pH 3, the Ni adsorption was 22 mg/g and decreased to 13 mg/g as it reaches to 4.55 (Figure 3), the pH_{zpc}. The exchange of protons and Ni ions on the biofilm surface may be the reason behind high adsorption at pH 3.0. With the increase in pH values greater than 4.55, the adsorption showed an increment with

TABLE 1 Physiochemical Parameters of the Biofilm

Parameter	Value
pH of the biofilm	3.5
Total acidic groups (μmol g^{-1})	2702
Total basic groups (μmol g^{-1})	1994
Carboxylic groups (μmol g^{-1})	46
Lactonic groups (μmol g^{-1})	552
Phenolic groups (μmol g^{-1})	2103

the increase of pH. Adsorption showed a maximum of 41.02 mg/g at pH 9.0. This could be explained as electrostatic attraction of Ni ions to the negatively charged surface of the biofilm beyond the pH_{zpc}.

Biosorption Isotherm Experiments

Maximum adsorption of 100 mg/g was reached at initial Ni concentration of 500 mg/L (Figure 4a). With the increase in the initial Ni concentration, the uptake increased; however, the removal percentage decreased. For instance, on changing the initial Ni concentration from 25 to 500 mg/L, the amount of biosorbed Ni increased from 3.43 to 38.16 mg/g, but the removal percentage decreased from 12.36% to 6.87%. This could be explained as at lower concentrations, the ratio of the initial moles of Ni to the available surface area is low and subsequently the fractional sorption is independent of the initial concentrations (Quintelas et al. 2008). On the other hand, the available sites become fewer compared with the number of molecules of Ni present at higher concentrations. Therefore, the removal percentage of Ni depends on the initial concentration.

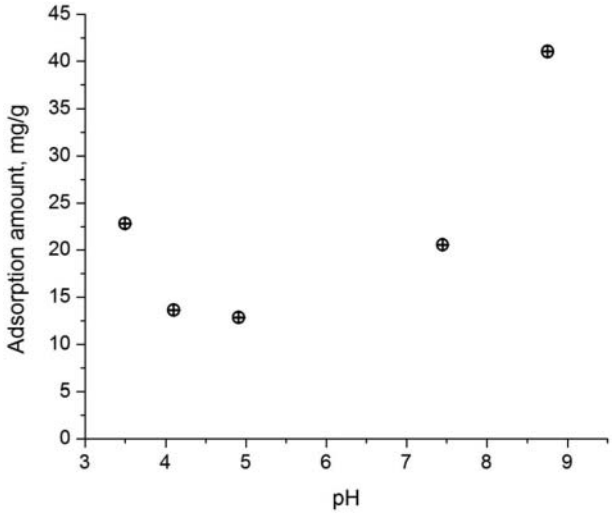

FIGURE 3 Dependence of Ni adsorption capacity with pH of the medium. Initial concentration used was 500 mg/L.

Experimental data were fitted to a number of isotherm models (Hill, Langmuir, Freundlich, Redlich and Peterson, Temkin, and Dubinin-Raduskevich [DR]) in order to understand the mechanism of Ni bioremoval (Figure 4a). The data were best fitted with the Hill model, with $R^2 = .988$ (Table 2). In the Hill model of adsorption, it is also considered as homogeneous like Langmuir and the adsorption is treated as a cooperative process due to adsorbate-adsorbent interactions (Ringot et al. 2007). Hence, a cooperative Ni sorption can be proposed for the studied microbial biofilm. The Langmuir model quantitatively describes the formation of a monolayer adsorbate on the outer surface of the adsorbent. Thereby, the Langmuir model represents the equilibrium distribution of metal ions between the solid and liquid phases, assuming that all adsorption sites have equal affinity for the adsorbate and therefore only monolayer adsorption occurs. Langmuir separation factor, K_R, indicates the adsorption nature to be either unfavorable ($K_R > 1$), linear ($K_R = 1$), favorable ($0 < K_R < 1$), or irreversible ($K_R = 0$). Langmuir separation factor ($0 < K_R < 1$) indicated that Ni sorption is a favorable reaction with monolayer adsorption (Figure 4b), whereas the maximum adsorption capacity (Q_{max}) was determined to be 235.54 mg/g, with $R^2 = .985$, showing that the reaction is well fitted to Langmuir adsorption isotherm.

The Freundlich isotherm is commonly used to describe the adsorption characteristics for the heterogeneous surfaces with different affinities. Unlike the Langmuir isotherm, the Freundlich isotherm does not imply a maximum adsorption capacity of the sorbent. It indicates favorability of the adsorption by the function n. If $n = 1$, then the partition between the two phases are independent of the concentration. Where $n < 1$, it indicates a favorable process, and if $n > 1$, the process is not favorable for adsorption (Tseng and Wu 2008). Since $n < 1$ ($n = 0.752$) in Freundlich isotherm, it is a favorable sorption process (Table 2). $R^2 = .975$ shows the validness of Freundlich isotherm with this study.

In general, for a given horizon, R^2 decreased in the order Hill > Langmuir > Freundlich > Redlich-Peterson > Temkin > DR. Among all the adsorption isotherm models studied, the Hill adsorption is the best-fitted model, with a correlation coefficient of .988. The

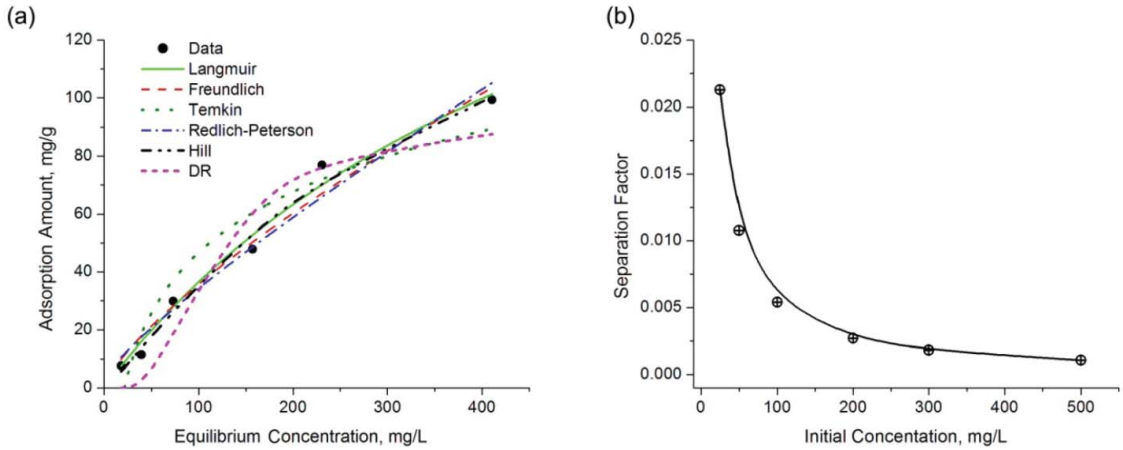

FIGURE 4 (*a*) **Experiment data of the Ni adsorption in different Ni concentrations. Symbols represent the experimental data, whereas the solid line represents calculated results using nonlinear least squares fit. (*b*) Plot of the Langmuir separation factor for the microbial biofilm with the initial Ni concentration at pH 5.**

Temkin model and DR model showed poor correlation coefficient values, indicating that these models did not fit with the experimental data.

Biosorption Kinetic Studies

The adsorption demonstrate an increase of the adsorption with the increase of time. After the adsorbate formed a thin monolayer over the surface, the capacity of the adsorbent decreased. Hence, the adsorption rate became constant and reached an equilibrium. In this study, the adsorption was gradually increased during the first 2 days (from 9.77 to 12.15 mg/g). A drastic increment of sorption was observed from the 2nd to the 4th day (from 12.15 to 29.87 mg/g). After 4 days, the adsorption rate reached an equilibrium, with a maximum sorption of ~30 mg/g for an initial concentration of 100 mg/L.

The adsorption kinetics of Ni at pH 4.5 was described by the first-order, second-order, pseudo-first-order, pseudo-second-order, simple Evolich, parabolic diffusion, and power function models. The first-order equation is often describes the reactions at the particle/solution interface. In the pseudo-first-order equation, a solid capacity is assumed from nondissociating molecular adsorption onto biosorbents. The pseudo-second-order adsorption kinetic rate equation is based on the assumption of chemisorption of the adsorbate on the adsorbents. The simple Elovich model is developed to describe the kinetics of heterogenous chemisorptions processes. The parabolic diffusion equation is often used to indicate rate-limiting diffusion-controlled phenomena. It successfully describes metal reactions on soils and soil constituents. Power function models are frequently used to describe rates of homogeneous chemisorption process (Sparks 1989).

With respect to the calculated values of correlation coefficient (R^2) and standard error of estimation (*SEE*), the power function can be considered as the best-fitted model (Table 3). This denotes that the interfacial interaction between Ni and the microbial biofilm or its EPS is homogeneous, which corroborates the fit to Hill and Langmuir isotherm modeling. The poorest fit of all with the experimental data was observed by pseudo-second-order equation. The equilibrium sorption data were satisfactorily fitted in the order of power function > pseudo-first-order > simple Elovich > parabolic diffusion > second-order > first-order > pseudo-second-order.

ATR-FTIR Analysis

FTIR analysis of the biofilm showed different functional groups that are responsible for the metal ion adsorption (Figure 5). Peaks characteristic to main functional groups of the microbial biofilm appeared at 1032, 1079, 1149, 1229, 1401, 1450, 1544, 1654, 1750, 2350, 2850, 2926, and 3384 cm^{-1}. The presence of many bands indicates the complex nature of the biofilm. The biofilm showed a broad and strong band in the region of 3200–3600 cm^{-1}, which could be ascribed to the presence of γO–H of the hydroxyl

TABLE 2 **Adsorption Isotherm Parameters for Ni at 1 g/L Biofilm**

Model	Equation	Description	Parameter	Value	Error	R^2	χ^2
Isotherm models							
Hill	$\Gamma_{ads} = \frac{\Gamma_{max}(K_L C_e)^a}{1+(K_L C_e)^a}$	a is the degree of interaction between adsorbent and adsorbate	K_L	0.003	0.002	.988	27.619
		Γ_{max} is the maximum sorption capacity	Γ_{max}(mg/g)	165.375	61.346		
			n	1.211	0.297		
Langmuir	$\Gamma_{ads} = \frac{\Gamma_{max} K_L C_e}{1+K_L C_e}$	Γ_{ads} is the amount of adsorbate adsorbed per unit area of surface (mol m^{-2}),	K_L	0.002	0.001	.985	24.573
		C_e is the equilibrium solution concentration (mol dm^{-3}) of adsorbate	Γ_{max}(mg/g)	235.540	55.626		
		K_L is the equilibrium constant for the overall adsorption process					
Freundlich	$\Gamma_{ads} = K_F C_e^n$	K_F((mg g^{-1})/(mg L^{-1})^n) is the Freundlich affinity-capacity parameter	K_F	1.119	0.525	.975	41.876
		n is the Freundlich exponent	n	0.752	0.082		
Redlich-Peterson	$\Gamma_{ads} = \frac{\Gamma_{max} C_e}{1+a_R C_e^{n_R}}$	a_R the Redlich-Peterson isotherm constant (dm^3 mol^{-1}), and	Γ_{max}(mg/g)	0.009	1.022	.969	69.513
		n_R is the Redlich-Peterson isotherm exponent	a_R	−1.003	0.636		
			n_R	−0.006	0.773		
Temkin	$\Gamma_{ads} = B \ln A_T + B \ln C_e$	B is the heat of adsorption, and	A_T	0.047	0.013	.919	135.725
		A_T is the binding constant (L mg^{-1})	B	81.867	12.190		
Dubinin-Raduskevicn	$\Gamma_{ads} = q_D \exp(-B_D[RT\ln(1+1/C_e)]^2$	R is the universal gas constant (8.314 J K^{-1} mol^{-1}), T is the absolute temperature	q_D	92.137	11.961	.889	185.947
		q_D is the adsorption capacity (mg g^{-1}), $B_D$is the mean free energy of sorption	B_D	0.001	0.001		
Other equations							
Separation factor	$K_R = \frac{1}{1+K_L C_e}$	K_L is the affinity constant	K_R	0.001–0.020			
Bonding energy for the ion-exchange mechanism	$E = \frac{1}{(2B_D)^{0.5}}$		E	22.36			
Gibbs free energy	$\Delta G_o = -RT\ln K_L$	R is universal gas constant (8.314 J mol^{-1} K^{-1})	ΔG_o	−1518.96			

TABLE 3 Kinetic Parameters of Ni Bioremoval in Biofilm Media

Model	Equation	Parameter		R^2	SEE
First order	$\ln(q_t) = \ln(q_0) - k_1 t$	k_1	0.2595	.8812	0.2116
		q_o	8.1571		
Second order	$\frac{1}{q_t} = \frac{1}{q_0} - k_2 t$	k_2	0.0149	.8831	0.0147
		q_o	9.3023		
Pseudo-first order	$\ln(q_e - q_t) = \ln(q_e) - k_1 t$	k_1	0.6919	.9235	0.4422
		q_e	61.8059		
Pseudo-second order	$\frac{t}{q_t} = \frac{1}{k_2 . q_e^2} + \left(\frac{1}{q_e}\right) t$	k_2	0.0001	.5139	0.0253
		q_e	85.4700		
Elovich	$q_t = \frac{1}{\beta}\ln(\alpha\beta) + \left(\frac{1}{\beta}\right)\ln t$	α	22.9958	.8881	3.9245
		β	0.0715		
Parabolic	$q_t = a + k_p t^{1/2}$	a	−12.5200	.8854	3.3296
		k_p	19.8310		
Power function	$\ln(q_t) = \ln(b) + k_f \ln(t)$	b	8.9155	.9250	0.1680
		k_f	0.7462		

group (Pagnanelli et al. 2012). The appearance of the band at 3384 cm^{-1} absorbance may be due to the N–H stretch of amine groups (Park et al. 2005). The absorption peak at 2926 cm^{-1} is ascribed to the asymmetric stretching of γC–H bond of the $-CH_2$ groups combined with that of the $-CH_3$ groups (Kazy, Das, and Sar 2006). A peak at 1750 cm^{-1} is due to the C=O stretching of carbonyl of carboxylic and ester groups (Yun et al. 2001). In the bare biofilm spectrum, the γC=O of amide I and δNH/γC=O combination of the amide II bond were present at 1654 and 1544 cm^{-1}, respectively, indicating the presence of carboxyl groups (Kazy, Das, and Sar 2006). The strong band that appeared at 1078 cm^{-1} is attributable to phosphate groups, whereas the peaks at 1032–1229 cm^{-1} are due to the presence of C–O group in ether (Figure 5). In the control spectrum, the bands in between 1400 and 1500 cm^{-1} are due to the presence of the carboxyl groups (Kazy, Das, and Sar 2006). The bending vibrations of C–H in alkanes and the stretching are ascertained by the peak at 1401 and 1405 cm^{-1}, respectively.

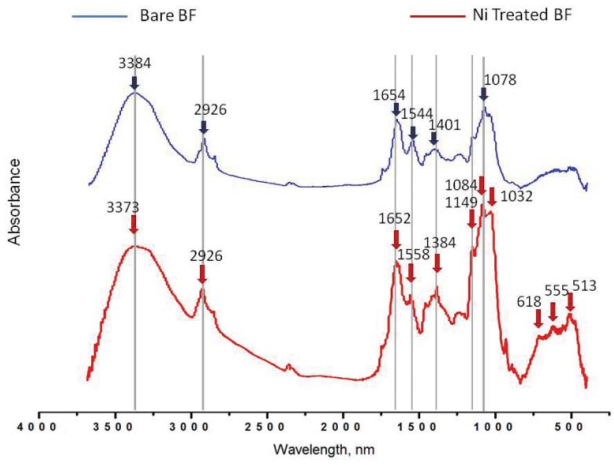

FIGURE 5 Changes in FTIR spectra of Ni-treated and not treated biofilms.

The FTIR spectra of Ni-loaded fungal-bacterial biofilm, in the range of 800–1700 cm^{-1}, were taken to confirm the presence of functional groups that are usually responsible for the biosorption process. An obvious change in the peak position and intensity at 1700–500 cm^{-1} region could be assigned to the formation of intense d(M–O) and d(O–M–O) bonds (M = metal ion) (Sar et al. 1999). A shift in peak position and more intensity in the spectrum of 3600–3200 cm^{-1} region in the Ni-loaded biofilm indicates the binding of Ni with amino and hydroxyl groups (Pradhan, Singh, and Rai 2007). Peak change at 1078 cm^{-1} shows the involvement of phosphate on Ni binding. A marked shift of the 1544 cm^{-1} peak to 1558 cm^{-1} region suggested a strong interaction of Ni with carboxyl groups (Kazy, Das, and Sar 2006). Following Ni sorption, the spectra exhibited a sharp increase in the peak intensities in between 1400 and 1500 cm^{-1}, indicating the strong role of carboxyl groups in Ni binding. Interestingly, in the Ni-loaded spectrum, the 1078 cm^{-1} peak has been split, forming three new peaks at 1032, 1084, and 1149 cm^{-1}, indicating strong role of phosphate in Ni binding (Figure 5). Also, the appearance of new peaks in 1000 and 500 cm^{-1} range may have been attributed to the phosphate interactions with Ni (Arai and Sparks 2001). In

general, the FTIR spectral analysis strongly supports the involvement of the carboxyl and phosphate groups in Ni binding by the microbial biofilm.

CONCLUSIONS

The behavior of the fungal-bacterial biofilm in Ni adsorbtion was investigated in this study. Microscopic and scanning electron microscopic images indicated prevalence of fungi in the microbial biofilm. Since the zero point charge of the biofilm was around pH 4.5, adsorption of Ni was more favorable at pH values greater than 4.5. Adsorption of Ni onto biofilm was studied with five different adsorption isotherm models, and the best-fitted model was the Hill model. Maximum Ni adsorption was calculated as 165 mg/g according to the Hill isotherm.

Biofilm-Ni interaction was found to be a monolayer homogenous adsorption with no interaction between adsorbate molecules on adjacent sites of the biofilm. The mechanism of adsorption is proposed as chemisorption, which involves sharing of electrons between adsorbent and adsorbate. Hence, Ni sorption by the biofilm seems to be strong due to the negatively charged acidic sites and the involvement of basic sites as observed by pH_{zpc} and Boehm data. The adsoption kinetics were very well described by the power function model. Since power function models are frequently used to describe rates of homogeneous chemisorption process, the chemisorption nature of the process is further confirmed. The FTIR spectral analysis of the biofilm before and after Ni adsorption showed the involvement of various functional groups such as carboxylic, ester, alkenyl, and phosphate on the adsorption process. The data indicate an efficient but slow removal of Ni by the microbial biofilm. Hence, this microbial biofilm may particularly be in the interest of contaminated soil remediation.

REFERENCES

Alves, S., M. Ascensão Trancoso, M. d. L. Simões Gonçalves, and M. M. Correia dos Santos. 2011. A nickel availability study in serpentinised areas of Portugal. *Geoderma* 164:155–163.

Arai, Y., and D. L. Sparks. 2001. ATR–FTIR spectroscopic investigation on phosphate adsorption mechanisms at the ferrihydrite–water interface. *J. Colloid Interface Sci.* 241:317–326.

Corcoll, N., B. Bonet, S. Morin, A. Tlili, M. Leira, and H. Guasch. 2012. The effect of metals on photosynthesis processes and diatom metrics of biofilm from a metal-contaminated river: A translocation experiment. *Ecol. Indicat.* 18:620–631.

Ferris, F. G., S. Schultze, T. C. Witten, W. S. Fyfe, and T. J. Beveridge. 1989. Metal interactions with microbial biofilms in acidic and neutral pH environments. *Appl. Environ. Microbiol.* 55:1249–1257.

Goertzen, S. L., K. D Thériault, A. M. Oickle, A. C. Tarasuk, and H. A. Andreas. 2010. Standardization of the Boehm titration. Part I. CO_2 expulsion and endpoint determination. *Carbon* 48:1252–1261.

Haghseresht, F., and G. Q. Lu. 1998. Adsorption characteristics of phenolic compounds onto coal-reject-derived adsorbents. *Energy Fuels* 12:1100–1107.

Hegazi, H. A. 2013. Removal of heavy metals from wastewater using agricultural and industrial wastes as adsorbents. *HBRC J.* 9:276–282.

Herath, H., A. U. Rajapaksha, M. Vithanage, and G. Seneviratne. 2014. Developed fungal–bacterial biofilms as a novel tool for bioremoval of hexavelant chromium from wastewater. *Chem. Ecol.* 30:418–427.

Jadhav, U. U, and H. Hocheng. 2014. Removal of nickel and cadmium from battery waste by a chemical method using ferric sulphate. *Environ. Technol.* 35:1263–1268.

Kazy, S. K., S. K. Das, and P. Sar. 2006. Lanthanum biosorption by a *Pseudomonas* sp.: Equilibrium studies and chemical characterization. *J. Ind. Microbiol. Biotechnol.* 33:773–783.

Krishnani, K. K., X. Meng, C. Christodoulatos, and V. M. Boddu. 2008. Biosorption mechanism of nine different heavy metals onto biomatrix from rice husk. *J. Hazard. Mater.* 153:1222–1234.

Liu, Y., M. C. Lam, and H. H. P. Fang. 2001. Adsorption of heavy metals by EPS of activated sludge. *Water Sci. Technol.* 43:59–66.

Ngwenya, B. T., I. W. Sutherland, and L. Kennedy. 2003. Comparison of the acid-base behaviour and metal adsorption characteristics of a gram-negative bacterium with other strains. *Appl. Geochem.* 18:527–538.

Oh, W.-C., and M.-H. Yum. 2004. Silver loading effect for the activated carbon fibers pre-treated with acid. *Bull. Korean Chem. Soc.* 25:1189–1194.

Omoike, A., and J. Chorover. 2004. Spectroscopic study of extracellular polymeric substances from bacillus s ubtilis: Aqueous chemistry and adsorption effects. *Biomacromolecules* 5:1219–1230.

Pagnanelli, F., C. Cruz Viggi, A. Cibati, D. Uccelletti, L. Toro, and C. Palleschi. 2012. Biotreatment of Cr(VI) contaminated waters by sulphate reducing bacteria fed with ethanol. *J. Hazard. Mater.* 199:186–192.

Park, S. S., D. Harrison, J. P. Pancras, and J. M. Ondov. 2005. Highly time-resolved organic and elemental carbon measurements at the Baltimore Supersite in 2002. *J. Geophys. Res. Atmos.* 110(D7). doi: 10.1029/2004JD004610.

Periasamy, K., and C. Namasivayam. 1995. Removal of nickel (II) from aqueous solution and nickel plating industry wastewater using an agricultural waste: Peanut hulls. *Waste Manage.* 15:63–68.

Pradhan, S., S. Singh, and L. C. Rai. 2007. Characterization of various functional groups present in the capsule of *Microcystis* and study of their role in biosorption of Fe, Ni and Cr. *Bioresour. Technol.* 98:595–601.

Quintelas, C., B. Fernandes, J. Castro, H. Figueiredo, and T. Tavares. 2008. Biosorption of Cr(VI) by a *Bacillus coagulans* biofilm supported on granular activated carbon (GAC). *Chem. Eng. J.* 136:195–203.

Quintelas, C., B. Fonseca, B. Silva, H. Figueiredo, and T. Tavares. 2009. Treatment of chromium (VI) solutions in a pilot-scale bioreactor through a biofilm of *Arthrobacter viscosus* supported on GAC. *Bioresour. Technol.* 100:220–226.

Quintelas, C., Z. Rocha, B. Silva, B. Fonseca, H. Figueiredo, and T. Tavares. 2009. Removal of Cd(II), Cr(VI), Fe(III) and Ni(II) from aqueous solutions by an *E. coli* biofilm supported on kaolin. *Chem. Eng. J.* 149:319–324.

Ringot, D., B. Lerzy, K. Chaplain, J.-P. Bonhoure, E. Auclair, and Y. Larondelle. 2007. In vitro biosorption of ochratoxin A on the yeast industry by-products: Comparison of isotherm models. *Bioresour. Technol.* 98:1812–1821.

Sar, P., S. K. Kazy, R. K. Asthana, and S. P. Singh. 1999. Metal adsorption and desorption by lyophilized *Pseudomonas aeruginosa*. *Int. Biodeterior. Biodegrad.* 44:101–110.

Seneviratne, G., R. M. M. S. Thilakaratne, A. P. D. A. Jayasekara, K. A. C. N. Seneviratne, K. R. E. Padmathilake, and M. S. D. L. De Silva. 2009. Developing beneficial microbial biofilms on roots of non legumes: A novel biofertilizing technique. In *Microbial strategies for crop improvement*, eds. M. S. Khan, A. Zaidi, and J. Musarrat, 51–62. Heidelberg, Germany: Springer.

Seneviratne, G., M. L. M. A. W. Weerasekara, and J. S. Zavahir. 2010. Microbial biofilms: How effective in rhizobium–legume symbiosis? In *Microbes for legume improvement*, eds. M. S. Khan, A. Zaidi, and J. Musarrat, 123–136. Vienna: Springer.

Seneviratne, G., J. S. Zavahir, W. M. M. S. Bandara, and M. L. M. A. W. Weerasekara. 2008. Fungal-bacterial biofilms: Their development for novel biotechnological applications. *World J. Microbiol. Biotechnol.* 24:739–743.

Sewwandi, B. G. N., M. Vithanage, S. S. R. M. D. H. R. Wijesekara, A. U. Rajapaksha, D. G. L. M. Jayarathna, and M. I. M. Mowjood. 2012. Characterization of aqueous Pb (II) and Cd (II) biosorption on native and chemically modified *Alstonia macrophylla* saw dust. *Bioremediat. J.* 16:113–124.

Sparks, D. L. 1989. *Kinetics of soil chemical processes*. New York: Academic Press.

Texier, A.-C., Y. Andrès, and P. Le Cloirec. 1999. Selective biosorption of lanthanide (La, Eu, Yb) ions by *Pseudomonas aeruginosa*. *Environ. Sci. Technol.* 33:489–495.

Toner, B., A. Manceau, M. A. Marcus, D. B. Millet, and G. Sposito. 2005. Zinc sorption by a bacterial biofilm. *Environ. Sci. Technol.* 39:8288–8294.

Trakal, L., R. Šigut, H. Šillerová, D. Faturíková, and M. Komárek. 2014. Copper removal from aqueous solution using biochar: Effect of chemical activation. *Arabian J. Chem.* 7:43–52.

Tseng, R.-L., and F.-C. Wu. 2008. Inferring the favorable adsorption level and the concurrent multi-stage process with the Freundlich constant. *J. Hazard. Mater.* 155:277–287.

Vithanage, M., A. U. Rajapaksha, C. Oze, N. Rajakaruna, and C. B. Dissanayake. 2014. Metal release from serpentine soils in Sri Lanka. *Environ. Monit. Assess.* 186:3415–3429.

Yee, N., and J. Fein. 2001. Cd adsorption onto bacterial surfaces: a universal adsorption edge? *Geochim. Cosmochim. Acta* 65:2037–2042.

Yun, Y.-S., D. Park, J. M. Park, and B. Volesky. 2001. Biosorption of trivalent chromium on the brown seaweed biomass. *Environ. Sci. Technol.* 35:4353–4358.